MODELING HYDRAULIC FRACTURING AND INDUCED SEISMICITY IN UNCONVENTIONAL RESERVOIRS USING MULTIPHASE FLUID-FLOW SIMULATIONS

Juan E. Santos

Instituto del Gas y del Petróleo, **Facultad de Ingeniería UBA** and Department of Mathematics, **Purdue University** and Universidad Nacional de La Plata

Work in collaboration with: L. A. Macias **(UBA)**, G. B. Savioli **(UBA)** and J. M. Carcione **(OGS)**

INTRODUCTION I

➤ Hydraulic fracturing or fracking consists in injecting fluids at high pressure into a reservoir in order to produce fractures or to connect already existing natural fractures, creating pathways where the hydrocarbons flow to the wellbore.

➤ This procedure is required in unconventional reservoirs because of their low permeability, as it is the case of tight gas, tight oil, shale gas or shale oil reservoirs.

➤ During the process of fluid injection into a reservoir the pore pressure builds up and, consequently, micro-seismic events along pre-existing zones of weakness may occur.

➤ Tracking these events can help to follow the evolution of the fractures along with its geometry.

INTRODUCTION II

➢ In this work, we employ a multiphase fluid flow numerical simulator to model the distribution of micro-seismic events caused by pore pressure increase during water injection in a gas reservoir.

➢ Given a spatial distribution of weak stress zones and a threshold pore pressure, the simulator predicts the spatio-temporal distribution of the micro-seismic events.

➢ The influence of different reservoir rock matrix properties and of the interacting fluids over the time-spatial distribution of these sources is analyzed.

➢ A wave propagation simulator is applied to monitor the evolution of the fracture network.

METHODOLOGY

➢ Use a Black-OIL multiphase fluid flow numerical simulator to model water injection in a gas reservoir.

➢ Apply a breakdown pressure criterion to determine the computational cells to be fractured and where the petrophysical properties must be updated.

➢ Analyze the microseismic event distribution.

➢ Use a numerical simulator of wave propagation in viscoelastic media to monitor the fracking procedure.

NUMERICAL MODEL OF WATER-GAS FLOW I

Mass conservation equation

$$-\nabla \cdot \left(\frac{1}{B_g} \bar{v}_g + \frac{R_s}{B_w} \bar{v}_w \right) + q_g = \frac{\partial \left[\phi \left(\frac{S_g}{B_g} + \frac{R_s S_w}{B_w} \right) \right]}{\partial t}$$

$$-\nabla \cdot \left(\frac{1}{B_w} \bar{v}_w \right) + q_w = \frac{\partial \left[\phi \frac{S_w}{B_w} \right]}{\partial t}$$

$$w \longrightarrow \text{water} \quad g \longrightarrow \text{gas}$$

Darcy's Empirical Law

$$\bar{v}_g = -\bar{\bar{K}} \frac{k_{rg}}{\eta_g} \left(\nabla p_g - \rho_g g \nabla z \right)$$

$$\bar{v}_w = -\bar{\bar{K}} \frac{k_{rw}}{\eta_w} \left(\nabla p_w - \rho_w g \nabla z \right)$$

$$S_w + S_g = 1 \qquad p_g - p_w = P_C(S_w)$$

ϕ: porosity

S_i: phase i saturation

p_i: phase i pressure

q_i: flow rate per unit volume

R_s: gas solubility in water

B_g: gas formation volume factor

B_w: water formation volume factor

η_i: phase i viscosity

$\bar{\bar{K}}$: absolute permeability tensor

$k_{ri}(S_i)$: phase i relative permeability

$P_C(S_i)$: gas-water capillary pressure

NUMERICAL MODEL OF WATER-GAS FLOW II

➢ The numerical solution is obtained employing the public domain software BOAST.

➢ BOAST solves the flow differential equations using IMPES (IMplicit Pressure Explicit Saturation), a finite difference technique.

➢ The basic idea of IMPES is to solve:

  ✓ A pressure equation obtained combining the flow equations for both phases.
  ✓ A saturation equation, which is the flow equation for the water phase.

IMPES TECHNIQUE I

Pressure equation

$$B_g \left[\nabla \cdot \left(\bar{\kappa} \left(\frac{k_{rg}}{B_g \eta_g} (\nabla p_w - \rho_g g \nabla D) + \frac{R_s k_{rw}}{B_w \eta_w} (\nabla p_w - \rho_w g \nabla D) + \frac{k_{rg}}{B_g \eta_g} \nabla P_C \right) \right) \right]$$

$$+ (B_w - R_s B_g) \left[\nabla \cdot \left(\bar{\kappa} \frac{k_{rw}}{B_w \eta_w} (\nabla p_w - \rho_w g \nabla D) \right) \right] + \frac{B_g q_g}{\rho_g^{SC}} + (B_w - R_s B_g) \frac{q_w}{\rho_w^{SC}} = \Phi c_t \frac{\partial p_w}{\partial t}$$

Total compressibility

Saturation equation

$$\nabla \cdot \left(\bar{\kappa} \frac{k_{rw}}{B_w \eta_w} (\nabla p_w - \rho_w g \nabla D) \right) + \frac{q_w}{\rho_w^{SC}} = \frac{\partial \left[\Phi \frac{S_w}{B_w} \right]}{\partial t}$$

IMPES TECHNIQUE II

➢ The system is linearized evaluating the pressure and saturation dependent coefficients at the previous time step.

➢ The pressure equation is solved implicitly, applying a Block Successive Over Relaxation method (BSOR) to compute the linear system solution.

➢ The saturation equation is solved explicitly, therefore stability restrictions are considered to select the time step.

FRACTURE CRITERION

➢ To simulate fracture propagation, we apply a criterion based on a "Breakdown Pressure", which is computed from the horizontal stresses and the tensile stress of the rock (Economides, 1994):

$$P_{bd}(x, y, z) = 3\sigma_{Hmin}(x, y, z) - \sigma_{Hmax}(x, y, z) + T_0(x, y, z) - p_H(x, y, z)$$

σ_H: horizontal stress $- T_0$: rock stress $- p_H$: hydrostatic pressure

➢ Once cell pressure becomes greater than Breakdown Pressure on a certain grid cell, this cell is "fractured", i.e. the cell permeability is strongly increased.

➢ Consequently, the other petrophysical properties are updated following the relations described by Carcione's model.

PETROPHYSICAL PROPERTIES UPDATE

Carcione's model (Carcione et.al., IJRMMS, 2003)

$$p(t) = S_b p_b(t) + S_g p_g(t)$$

$$\frac{1 - \phi_c}{K_s}(p(t) - p_H) = \phi_0 - \phi(t) + \phi_c \ln\left(\frac{\phi(t)}{\phi_0}\right)$$

$$\frac{1}{k_x(t)} = \frac{45(1 - \phi(t))^2}{\phi(t)^3}\left(\frac{(1 - C)^2}{R_q^2} + \frac{C^2}{R_c^2}\right)$$

$$\frac{k_x(t)}{k_z(t)} = \frac{1 - (1 - 0.3a)\sin(\pi S_b)}{a(1 - 0.5\sin(\pi S_b))}$$

p: pore pressure

ϕ_c: critical porosity

R_q: radius of sand grains

R_q: radius of clay grains

K_s: bulk modulus of solid grains

a: permeability anisotropy parameter

C: clay content

ϕ_0: initial porosity

PROCEDURE
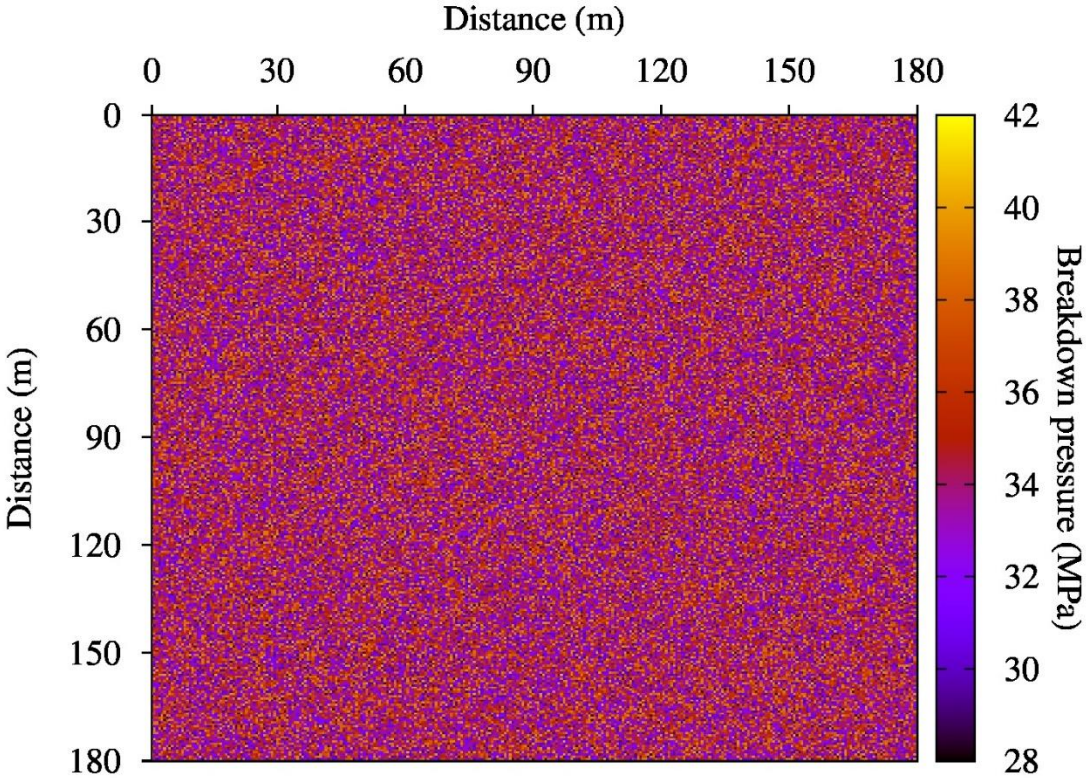
Breakdown Pressure fractal distribution

Pressure Map [MPa] → $p > P_{bd}$ → Fractured Cell → Permeability increase → Properties Update
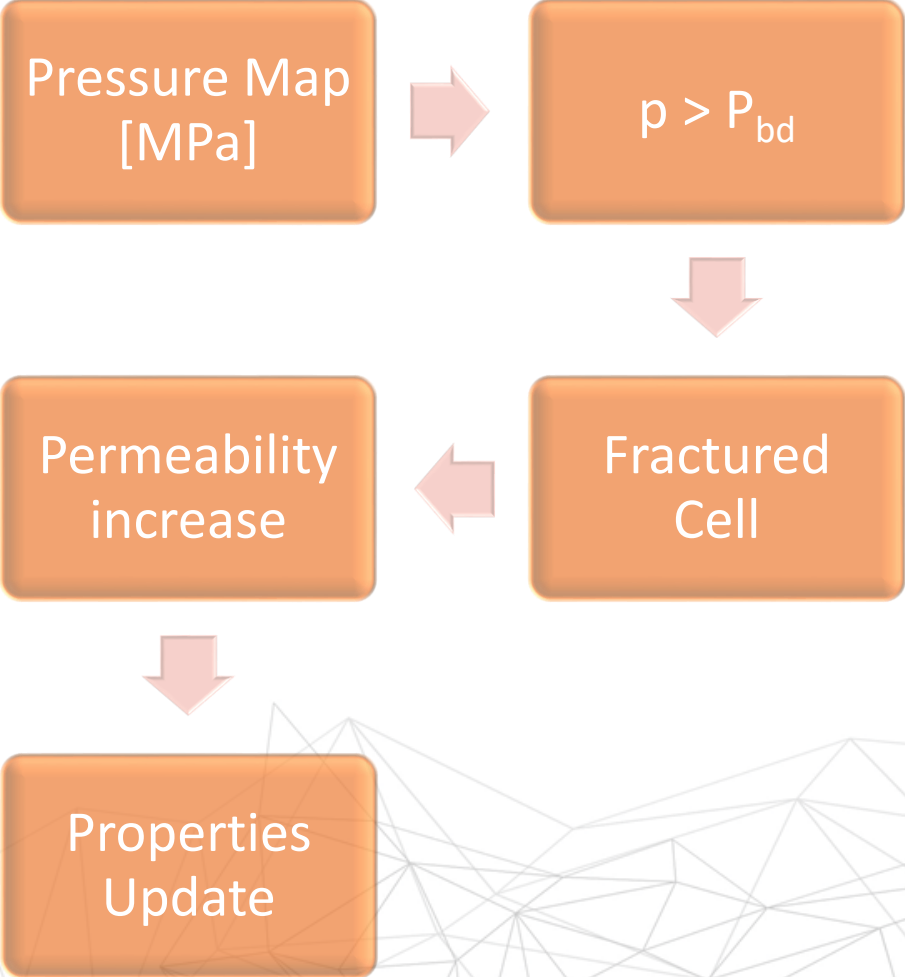
NUMERICAL EXPERIMENTS I

➢ Consider a 2D horizontal section in the x-y plane of a low permeability gas reservoir (0.1 mD) with an extent of 180 m x 180 m.

➢ The reservoir is located at 2500 m b.s.l., with 10% of initial porosity and 30% of initial water saturation. The data correspond to the Vaca Muerta formation.

➢ The simulation is performed by using a 300 × 300 uniform mesh.

➢ In the first experiment we assume that porosity and permeability are not modified when the breakdown pressure (P_{bd}) is reached.

➢ We also assume a fractal distribution of P_{bd} using the Von-Kármán correlation function (Frankel and Clayton, 1986).

➢ Water is injected at the center of the reservoir section with a constant flow rate of 0,15 m³/s.

NUMERICAL EXPERIMENTS II
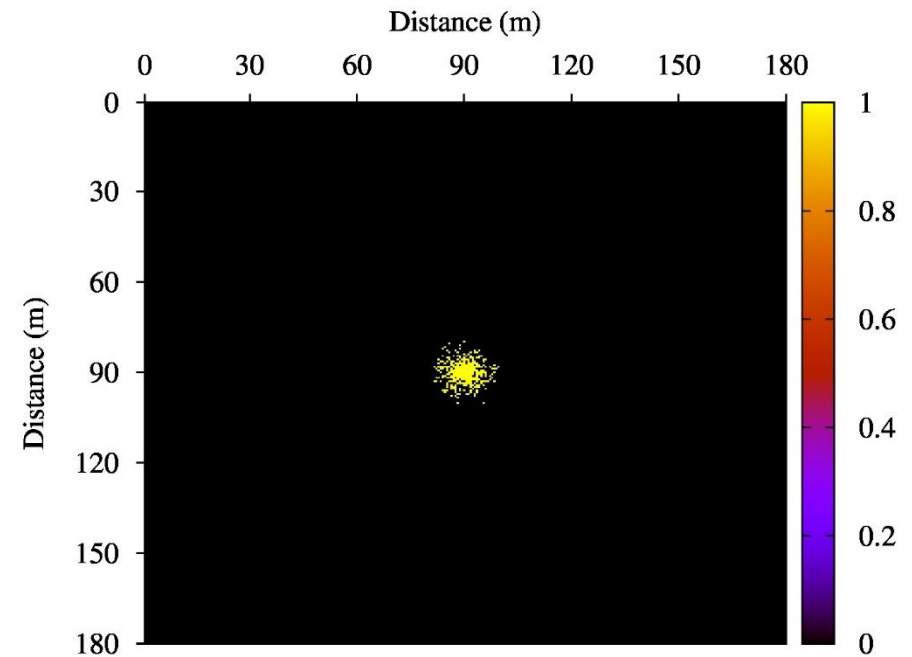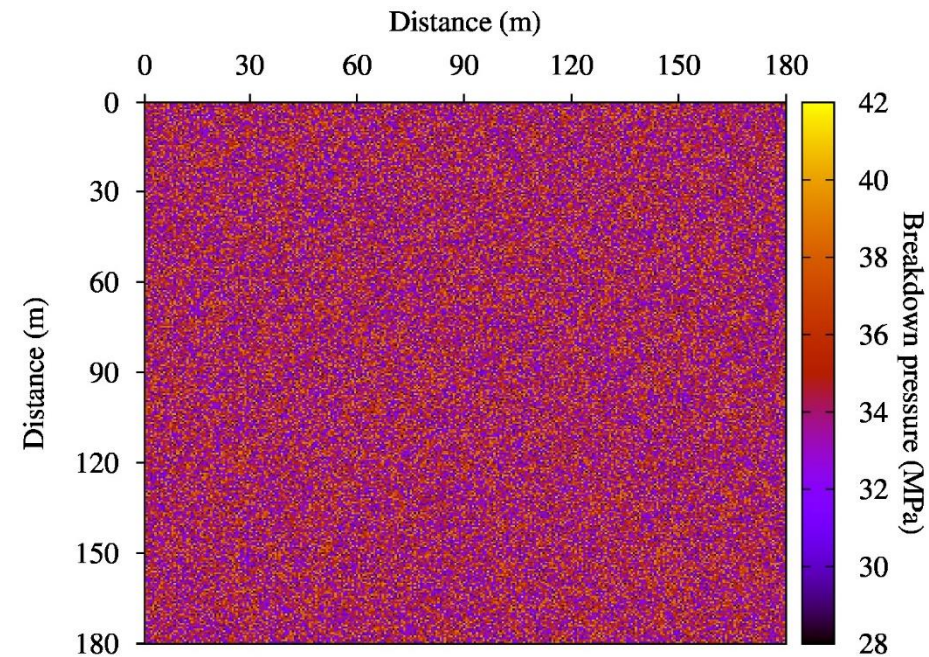
Left: fractal distribution for P_{bd} constructed with the Von-Kármán correlation function. Right: spatial distribution of micro-seismic sources after 10 h of the fracking process.

NUMERICAL EXPERIMENTS III
## Fractal versus constant breakdown pressure spatial distribution.
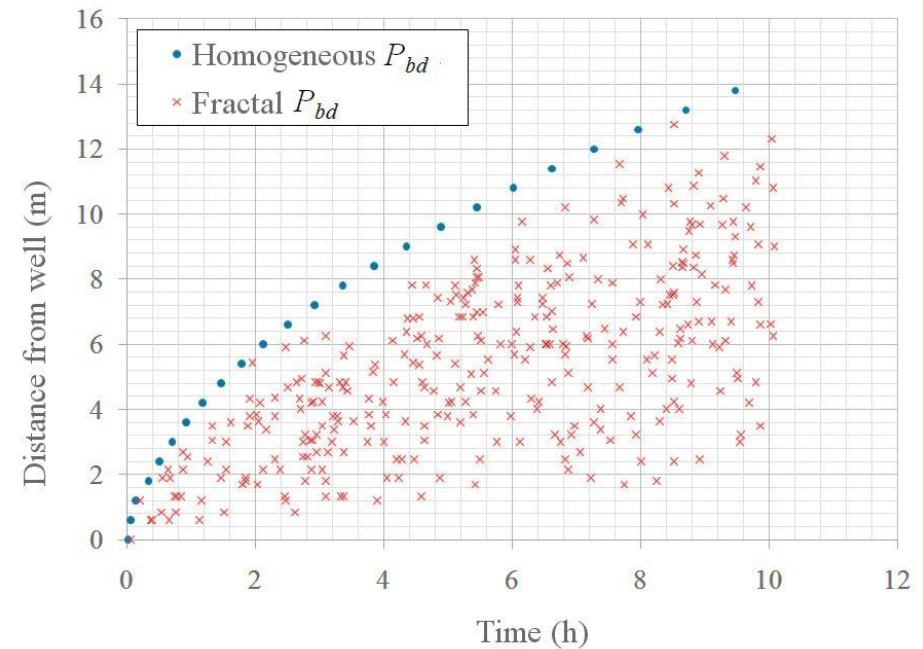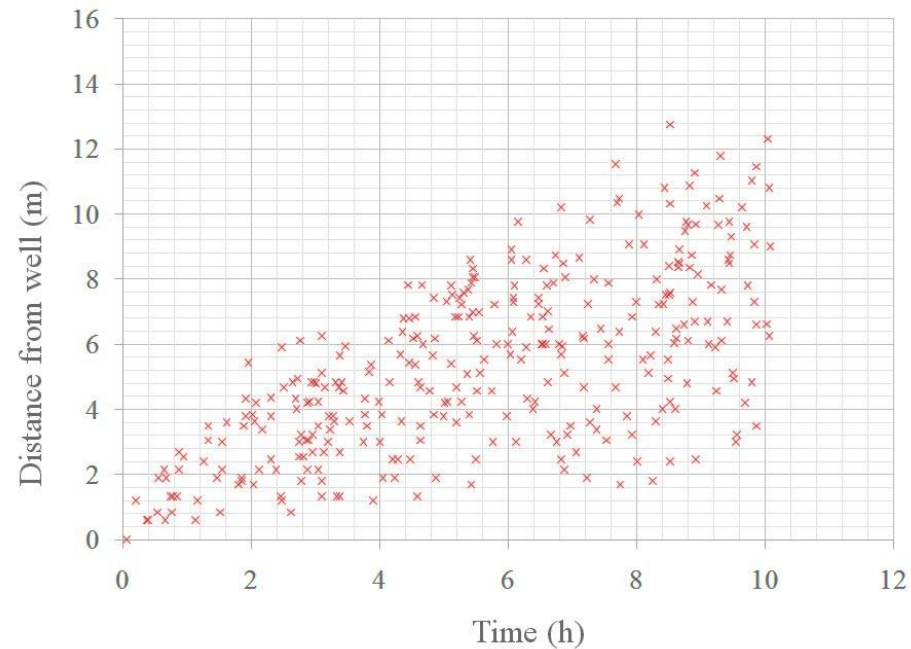
Left: Location of the microseismic events as a function of the emission time, corresponding to a fractal distribution of the breakdown pressure P_{bd}. Right: The envelope curve corresponds to a constant P_{bd} = 28 MPa, the minimum value of the fractal P_{bd}. This curve is the envelope of all microseismic events shown in the left Figure.

NUMERICAL EXPERIMENTS IV
The effect of updating porosity and permeability

Here we analyze the effect of increasing porosity and permeability values in a computational cell after the pore pressure reaches the P_{bd} value on that cell. An uniform value of P_{bd} of 28 MPa is assumed.
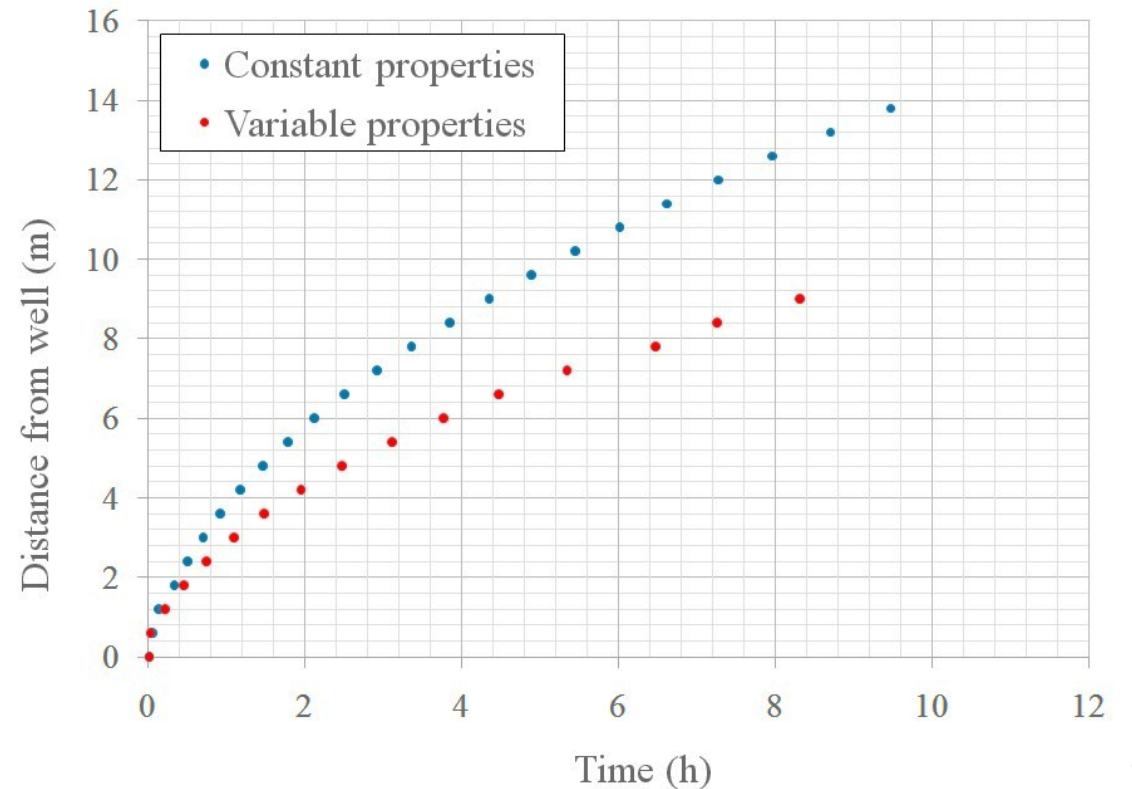
It can be observed that an increment in porosity and permeability produces a pressure drop. This decrease slows down the pressure front progress which, in turn, delays the triggers.

NUMERICAL EXPERIMENTS V
P_{bd} Sensitivity

Here we run four simulations for uniform spatial distributions of P_{bd} with values : 28, 31, 35 and 38 Mpa (4000, 4500, 5000, 5500 psi).
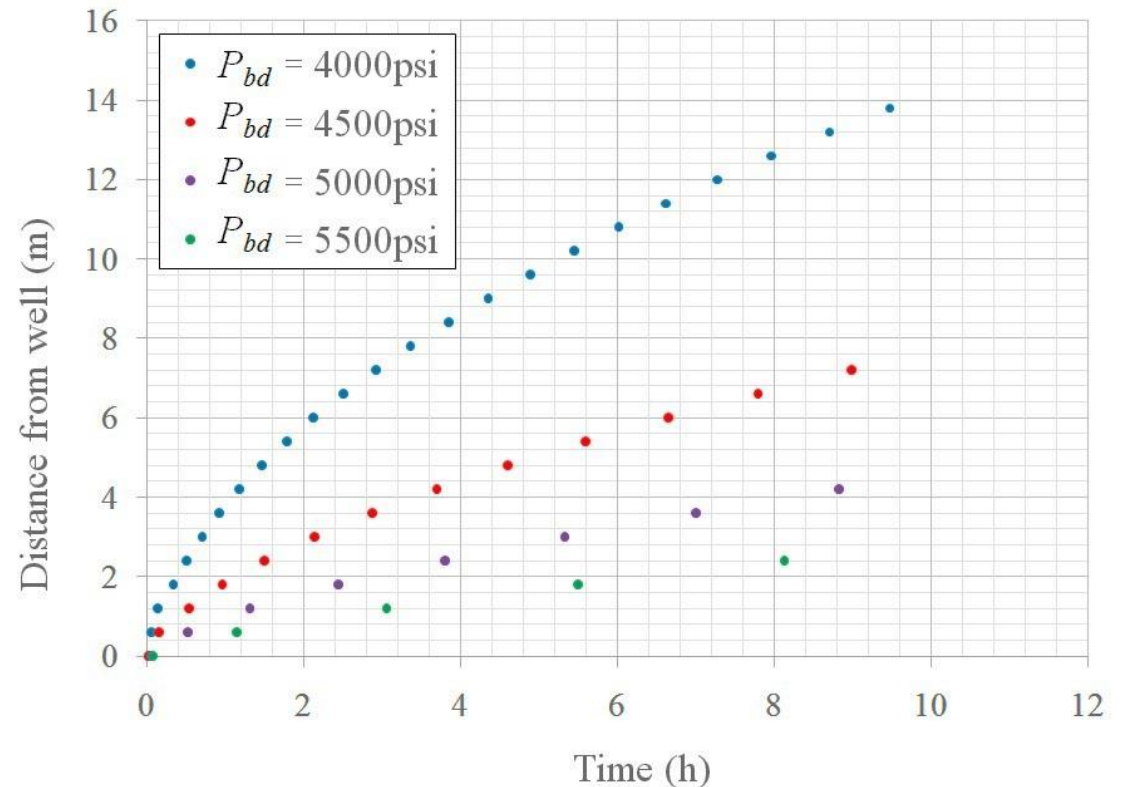
A P_{bd} increment slows down the occurrence of triggers and reduces the size of the fractured zone. This effect is due to the fact that for a given region, a higher P_{bd} value requires to reach a higher pore pressure to induce a fracture. An increase of about 12% on the P_{bd} induces a 50% decrease in the distance from the fracture front to the well.

NUMERICAL EXPERIMENTS VI
Initial water saturation sensitivity

In this experiments we run for five different initial water saturations Swi = 0.1, 0.3, 0.5, 0.8, 1.0. A constant P_{bd} of 28 MPa is assumed. The case S_{wi} = 1 corresponds to the single-fluid case usually assumed in the literature.
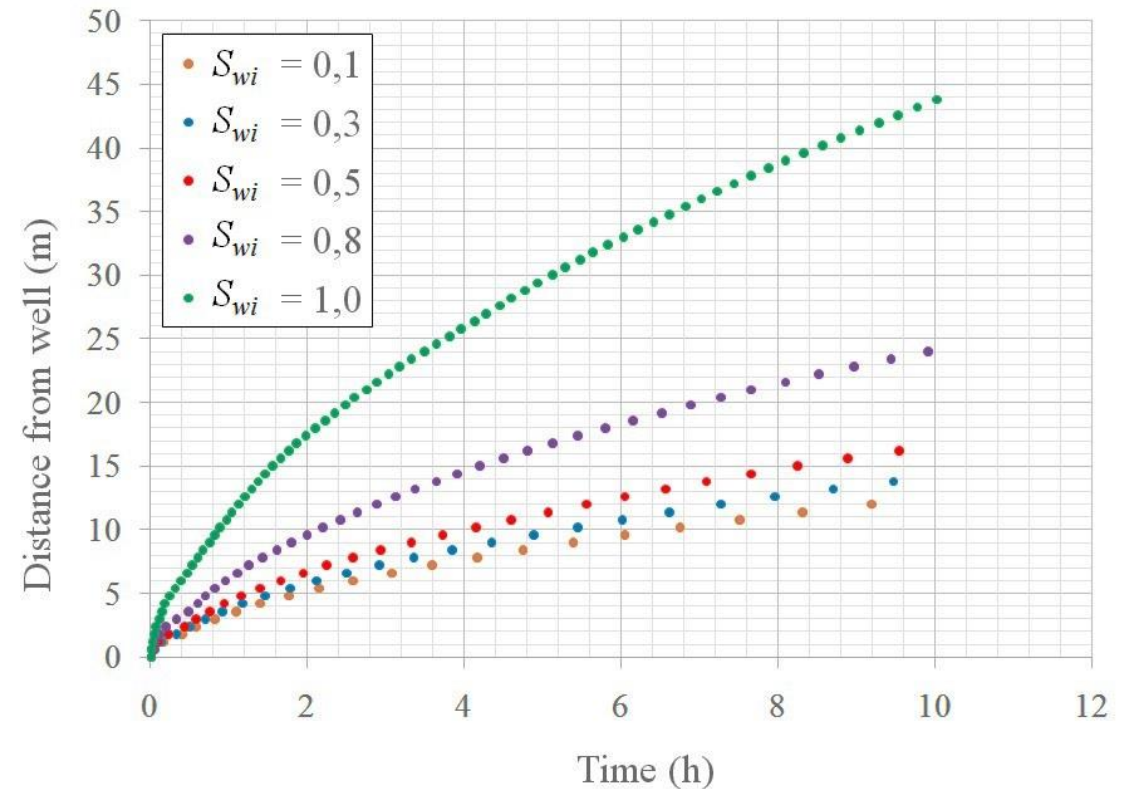

An increment of initial water saturation induces an acceleration of the evolution of the fracture front and an increasing of the fractured zone. This experiment shows the importance of considering two-phase fluid flow, because water injection into a gas reservoir greatly affects the trigger time evolution. This effect is mainly due to the difference in compressibility of the two phases.

NUMERICAL EXPERIMENTS VII

Pre-existing natural fractures effect

Here we analyze the case when the reservoir has natural fractures before starting the fracking process, and the influence of such natural fractures on the evolution of the induced fractures. Fractures are modeled as zones of high permeability (1 Darcy).
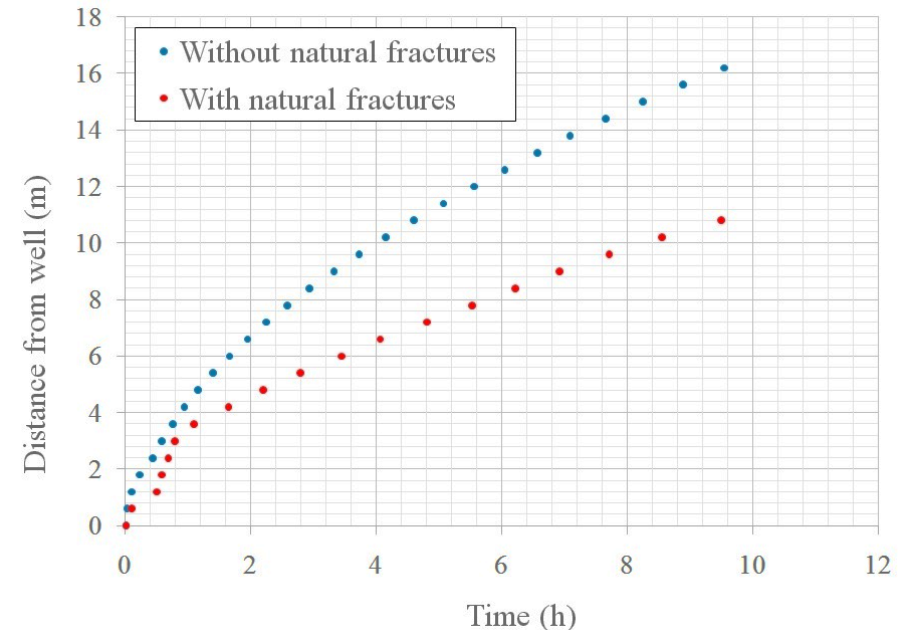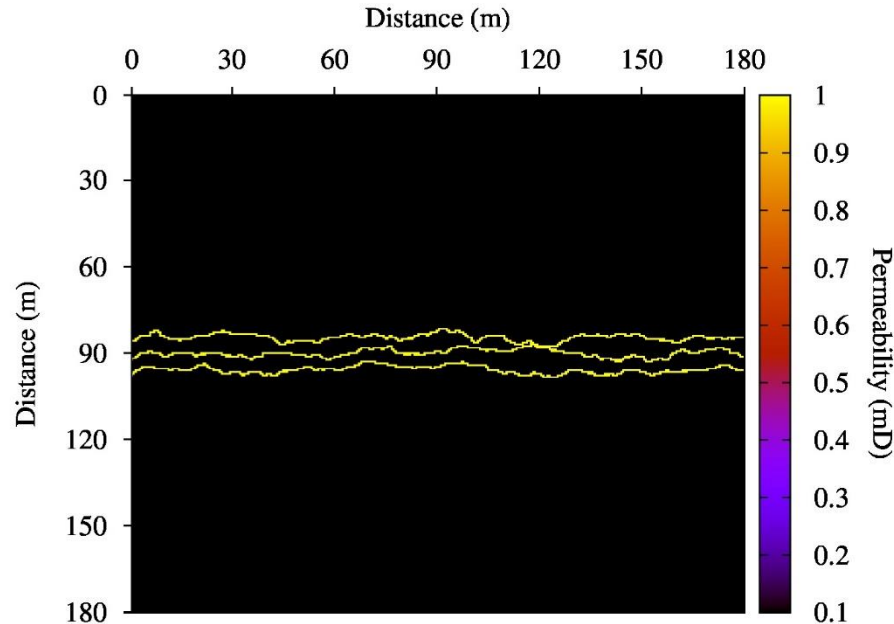

Left: Permeability map with natural fractures. Right: Effect of the natural fractures on the trigger distribution, where a decrease in the size of the fractured zone is observed. The natural fractures allows water to flow more easily, thus pressure increases slowly, which in turn decreases the number of induced fractures.

NUMERICAL EXPERIMENTS VIII
## Seismic monitoring of the fracking procedure

Here we study the seismic response obtained after a fracture process performed with 4 equally spaced injection points as the figure shows.

➤ For the fracking process simulation we apply an algorithm that allow us to obtained a random fracture distribution based on the breakdown pressure. A 0.75 m³/s rate of water is injected in each injection point.

➤ For the seismic monitoring we use a 2D simulator of wave propagation in viscoelastic media which includes mesoscopic attenuation effects using White's model. A 30 Hz point source is located on the left well and a line of 160 receivers in the right well.

➤ In numerical experiments we take a 2D vertical section in the x-z plane of 300 m x 300 m discretized with a 300x300 uniform mesh.
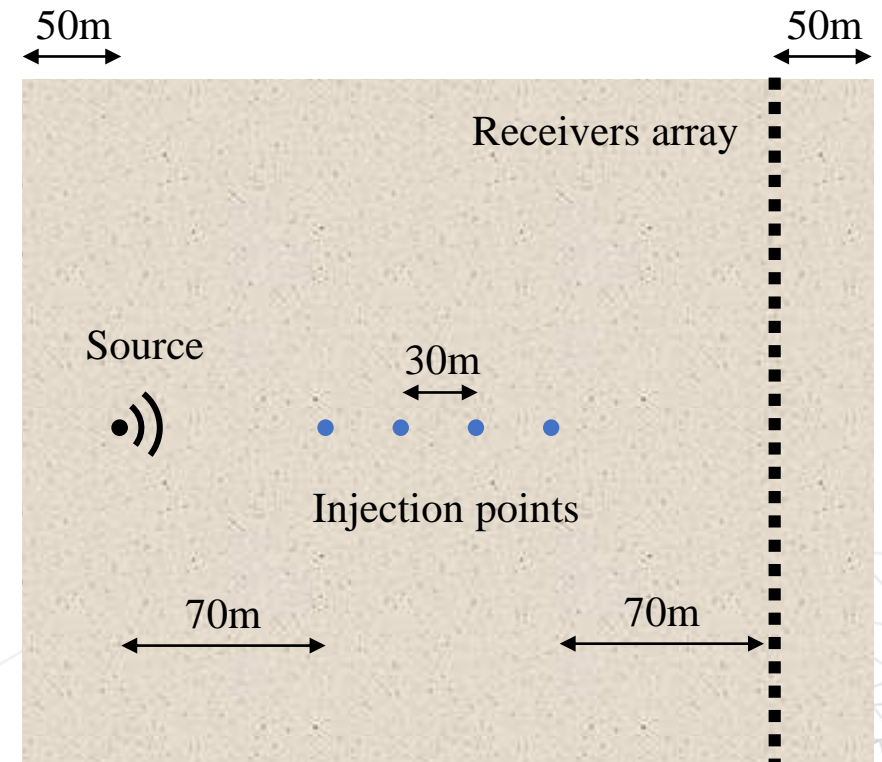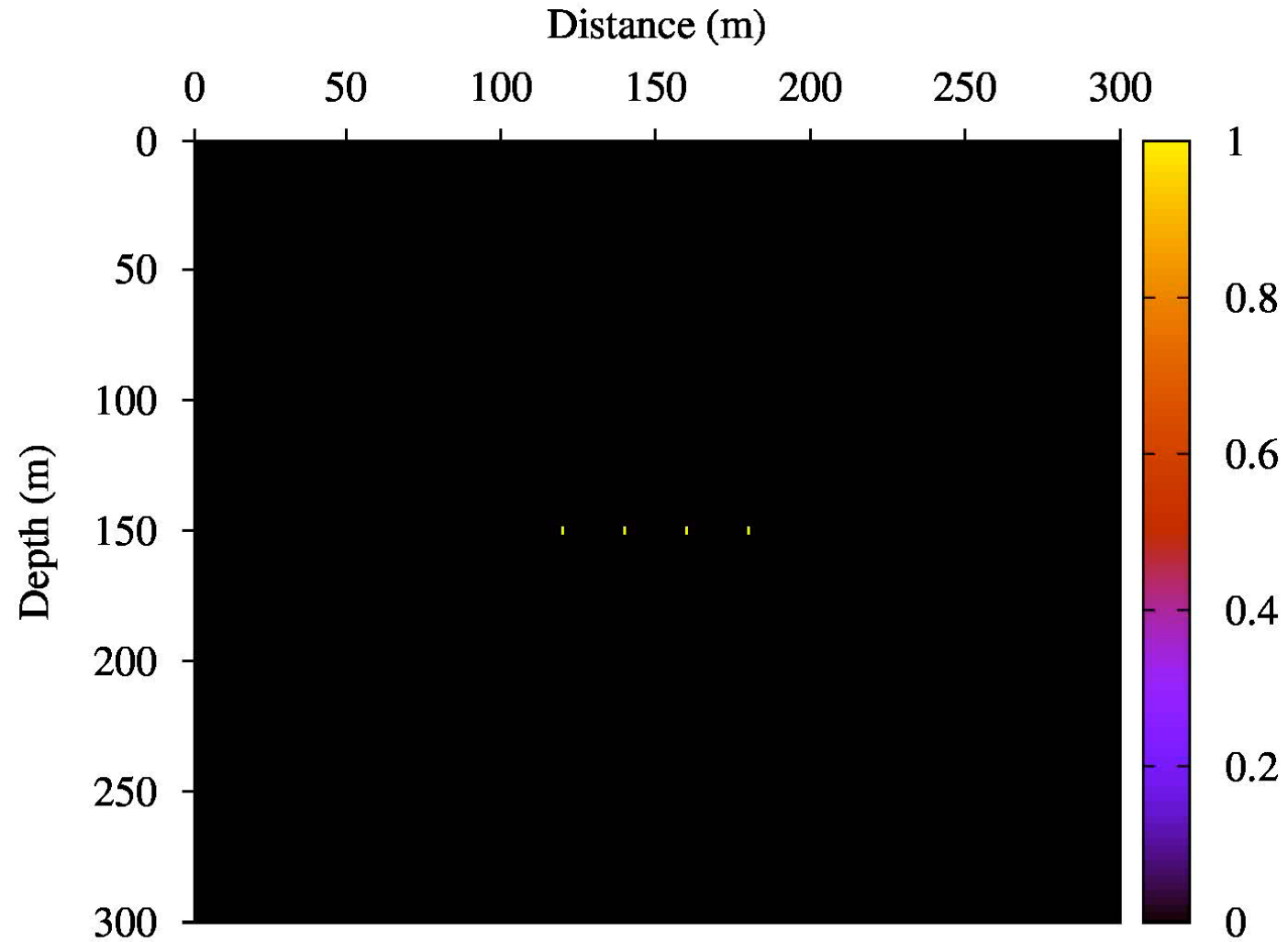
NUMERICAL EXPERIMENTS IX

Porosity and pore pressure maps
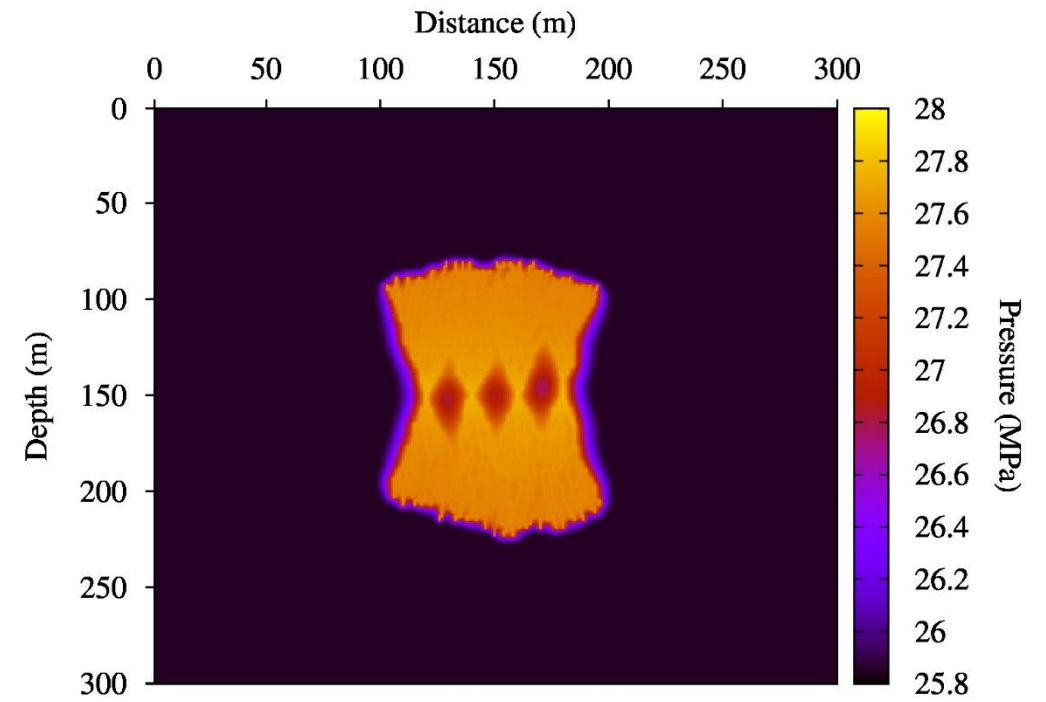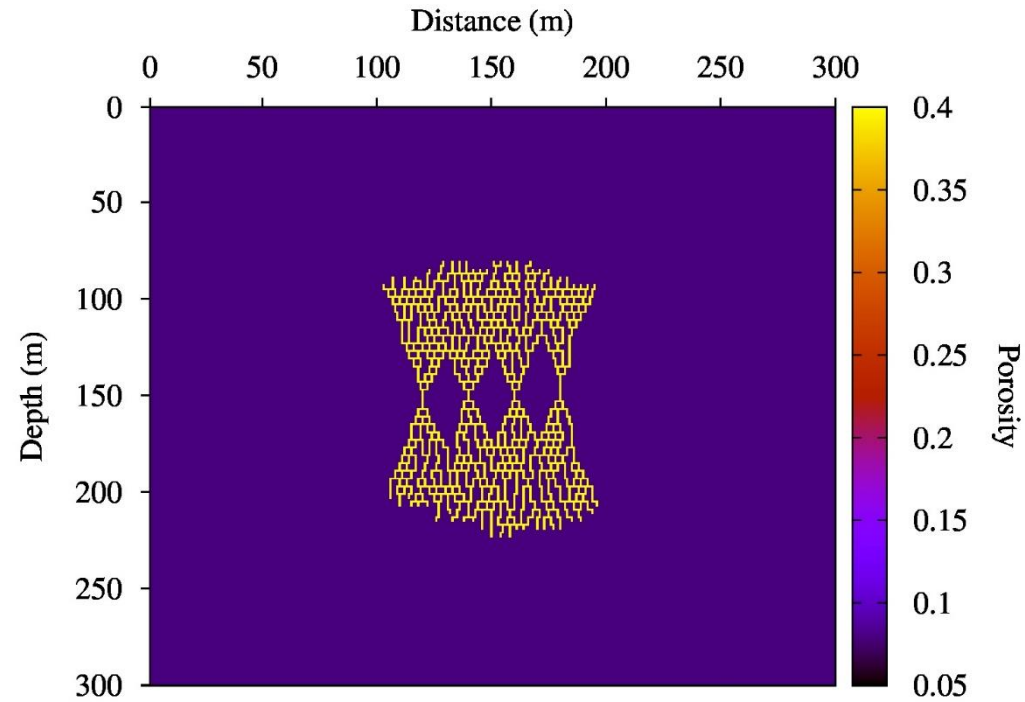
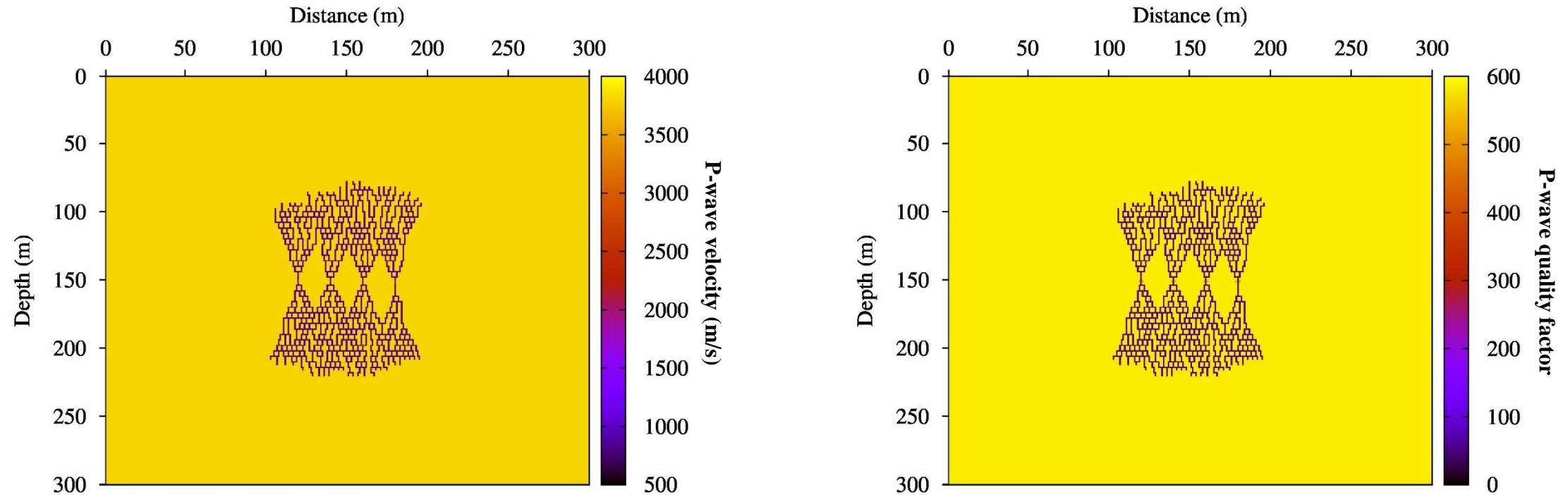Porosity map (left) and pressure map (right) after 10h of water injection.

NUMERICAL EXPERIMENTS X
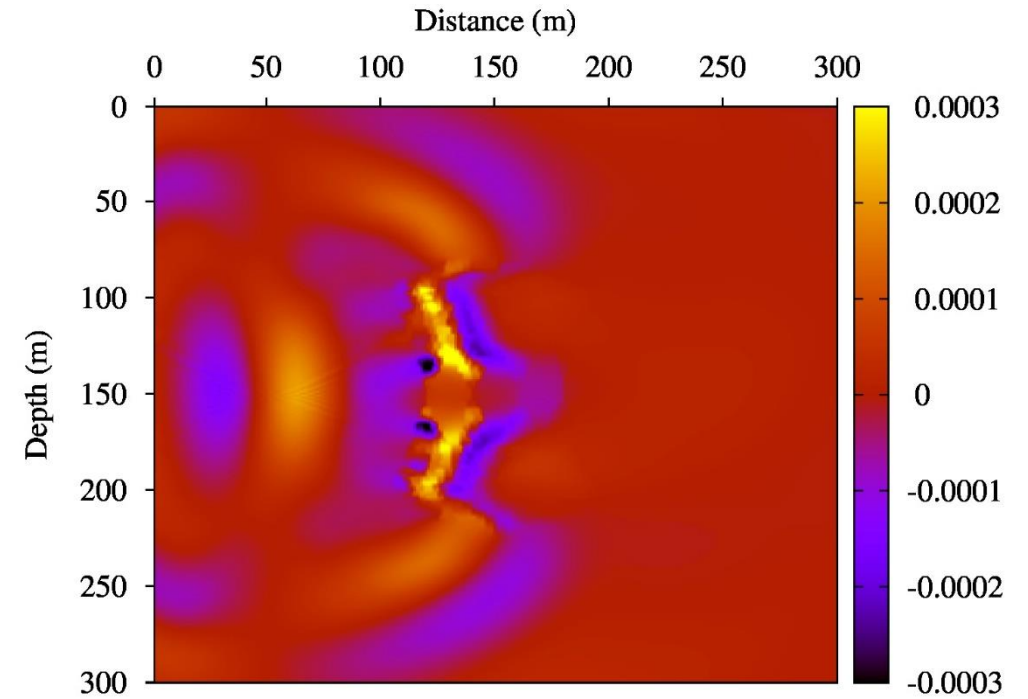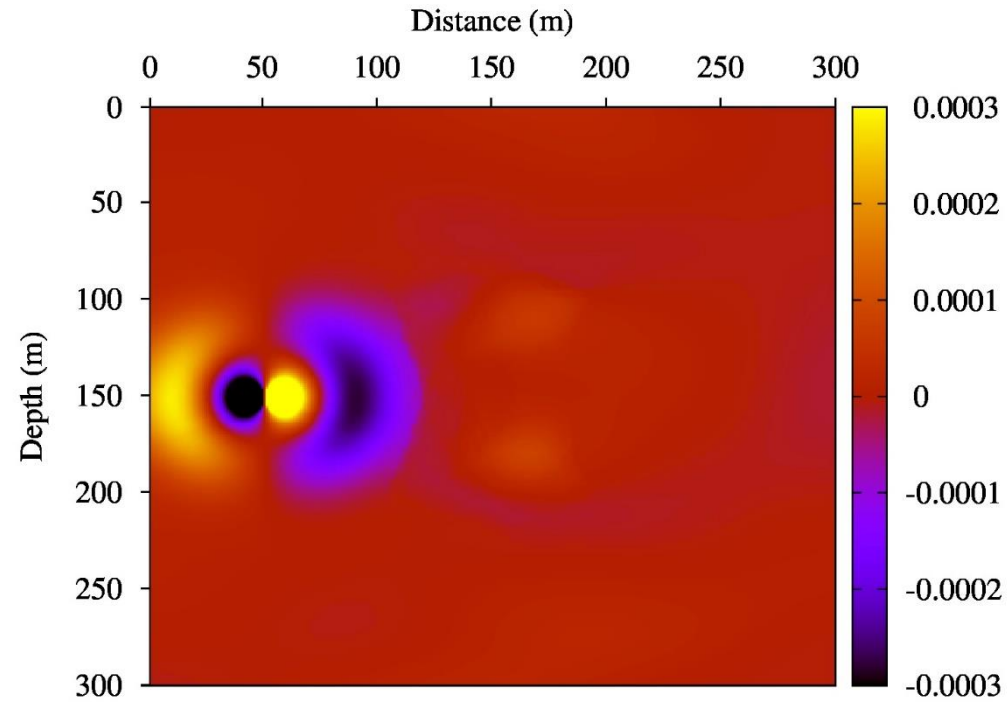
Fracture evolution

Velocity profile and Quality factor for P-waves

Velocity profile (left) and Quality factor (right). Note the decrease in P-wave velocity and Quality factors in the fractured zone.

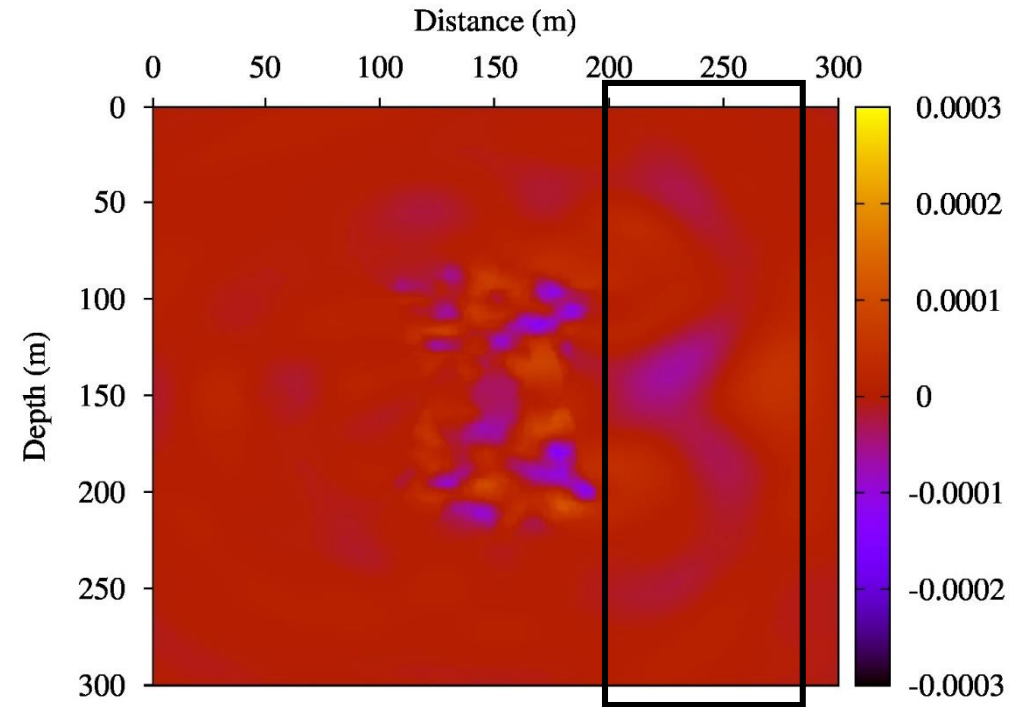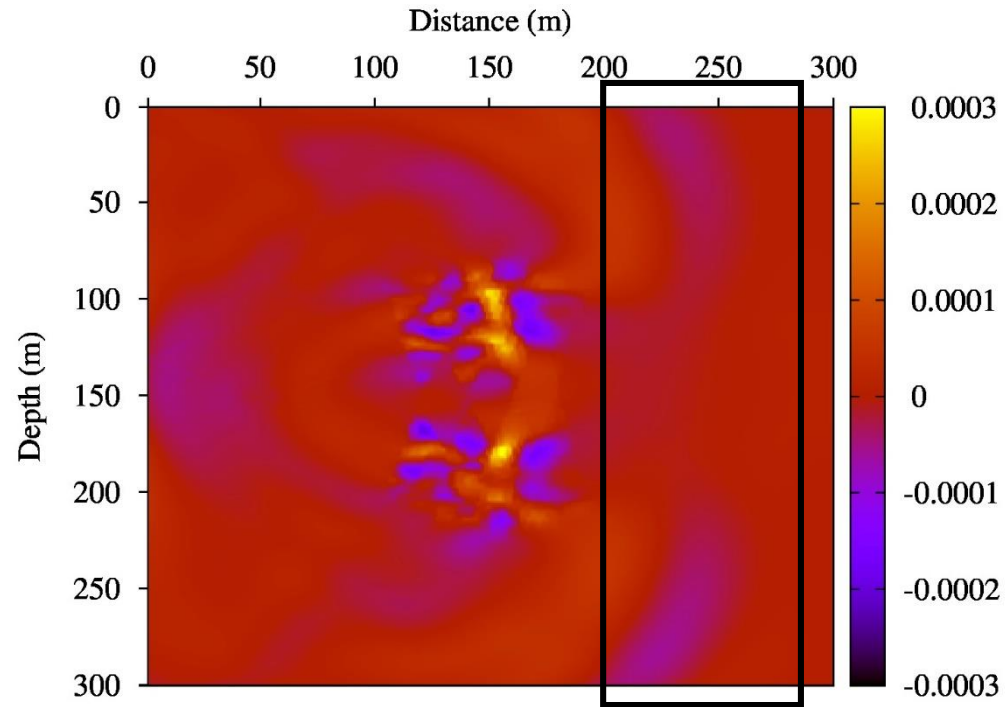# NUMERICAL EXPERIMENTS XIII
Snapshots of x-component of velocity

At 30 ms (left) the incident P-wave is arriving to the fractured zone. At 60 ms (right) the wavefront is travelling across the fractured zone, waves are being scattered and wave conversions are occurring.
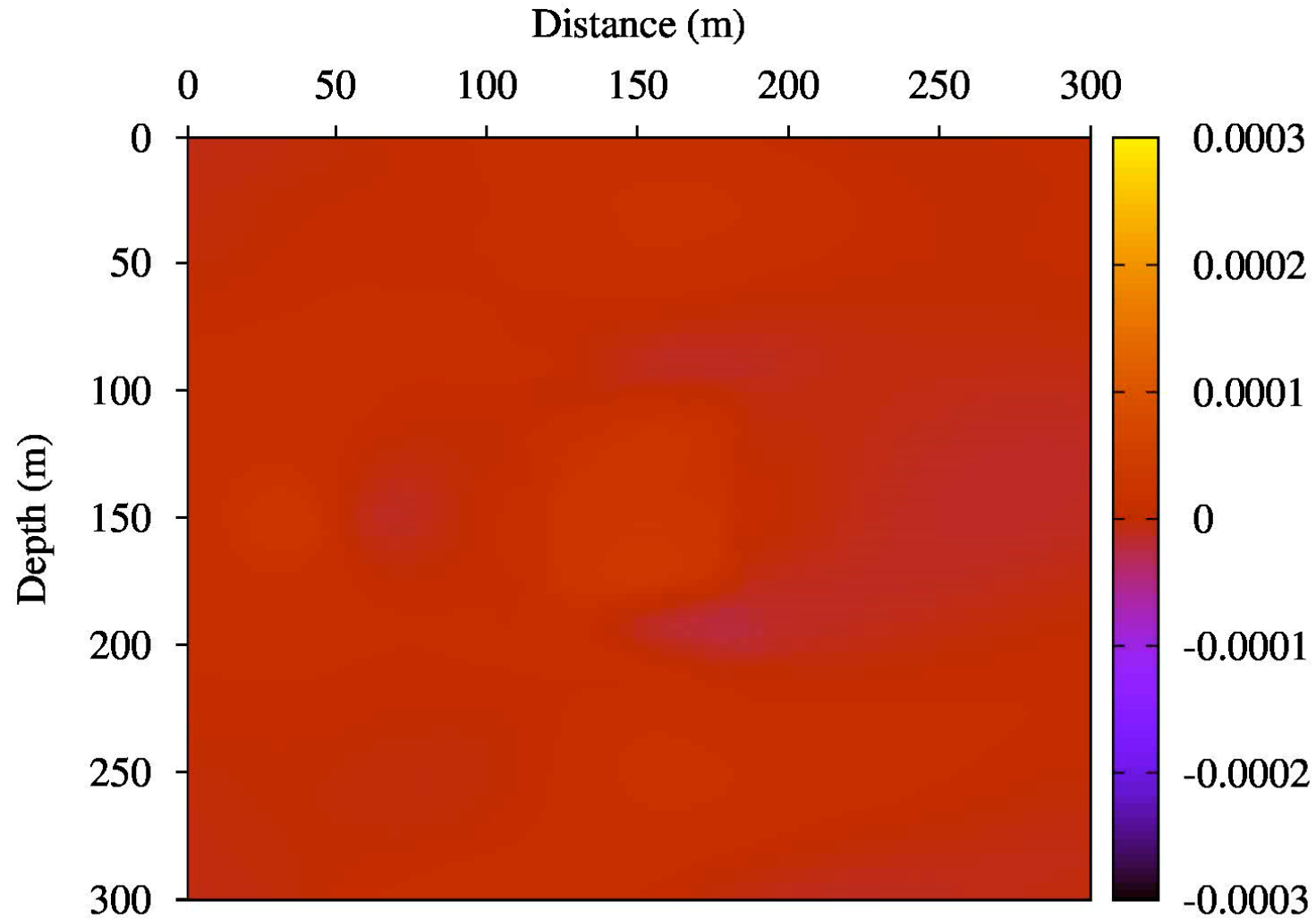
NUMERICAL EXPERIMENTS XIV
Snapshots of x-component of velocity

At 82ms (left) the first wave front is arriving to the receivers. At 135ms (right) the delayed wave front is arriving to the receivers.
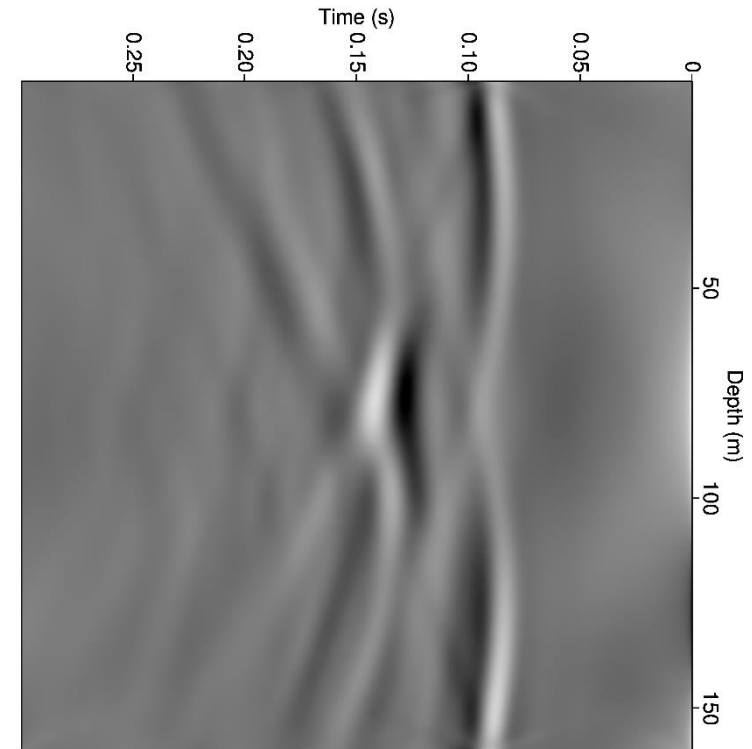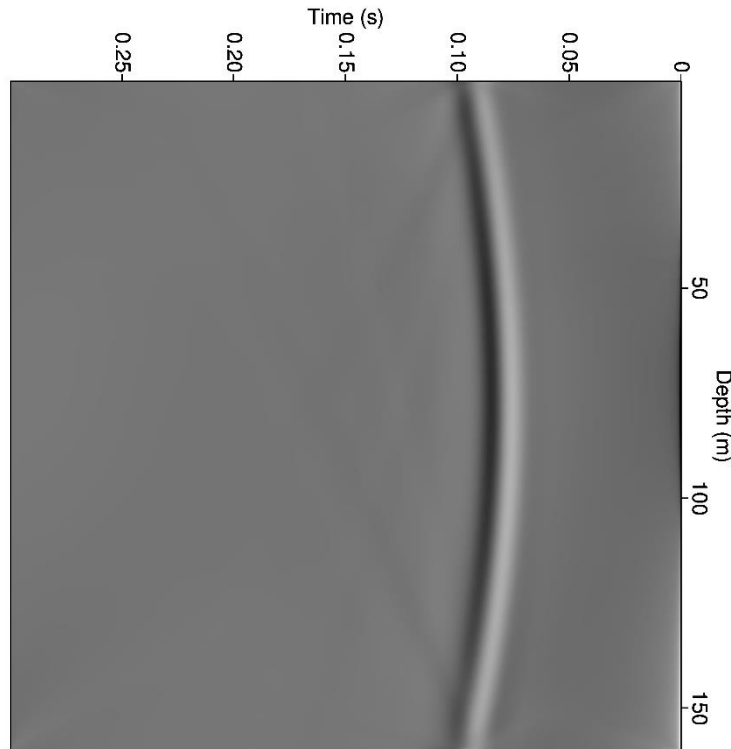
NUMERICAL EXPERIMENTS XV

X-component of velocity evolution

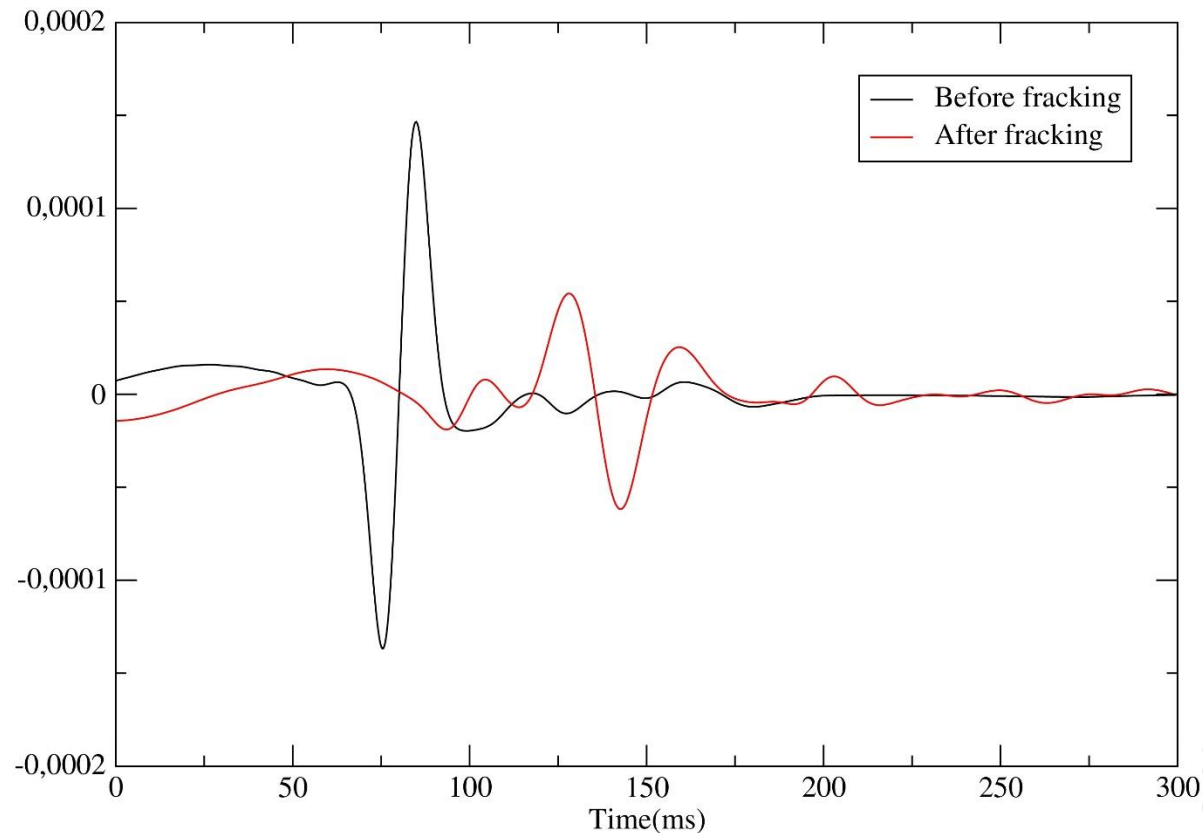# NUMERICAL EXPERIMENTS XVI

Synthetic seismogram observed at the well on the right

Note the delay at the center of the wave front due to the velocity decay within the fractured zone.

NUMERICAL EXPERIMENTS XVII

Synthetic traces before and after the fracking procedure

Traces at the receiver location (250m,150m) before and after injection. Note the delay of the P-wave arrival due to the decay in P-wave velocity in the fractured zone. This velocity change is associated with an increase in porosity and substitution of gas by water in the pore space.

CONCLUSIONS

➢ The numerical simulation examples have shown:

- ✓ A multiphase flow simulator is needed to properly model the generation and spatial distribution of the microseismic events as it was shown when considering different initial water saturations.
- ✓ The update of the porosity and permeability in the reservoir gives more realistic description of this phenomenon.
- ✓ The presence of natural fractures induces a reduction in the size of the fractured zone.
- ✓ An increase of breakdown pressure slows down the occurrence of triggers.

➢ The wave propagator simulator detected the presence of the fracture zone due to its changes in petrophysical properties and pore fluid saturations.

THANKS FOR YOUR ATTENTION!!!